



**HAL**  
open science

## Bone histology of *Iberosuchus macrodon* (Sebecosuchia, Crocodylomorpha)

Jorge Cubo, Meike Köhler, Vivian de Buffrénil

► **To cite this version:**

Jorge Cubo, Meike Köhler, Vivian de Buffrénil. Bone histology of *Iberosuchus macrodon* (Sebecosuchia, Crocodylomorpha). *Lethaia*, 2017, 19 (4), pp.495-503. 10.1111/let.12203 . hal-02295975

**HAL Id: hal-02295975**

**<https://hal.sorbonne-universite.fr/hal-02295975>**

Submitted on 24 Sep 2019

**HAL** is a multi-disciplinary open access archive for the deposit and dissemination of scientific research documents, whether they are published or not. The documents may come from teaching and research institutions in France or abroad, or from public or private research centers.

L'archive ouverte pluridisciplinaire **HAL**, est destinée au dépôt et à la diffusion de documents scientifiques de niveau recherche, publiés ou non, émanant des établissements d'enseignement et de recherche français ou étrangers, des laboratoires publics ou privés.

1 Bone histology of *Iberosuchus macrodon* (Sebecosuchia, Crocodylomorpha).

2

3 By

4 Jorge Cubo<sup>1\*</sup>, Meike Köhler<sup>2,3</sup>, Vivian de Buffrénil<sup>4</sup>

5

6 <sup>1</sup> Sorbonne-Universités, UPMC-Univ. Paris 06, CNRS, Institut des Sciences de la Terre de Paris  
7 (ISTeP), 4 place Jussieu, BC 19, 75005 Paris, France

8 <sup>2</sup> ICREA, Pg. Lluís Companys 23, 08010 Barcelona, Spain.

9 <sup>3</sup> Institut Institut Català de Paleontologia Miquel Crusafont, Universitat Autònoma de Barcelona,  
10 Carrer de les Columnes s/n, 08193 Cerdanyola del Vallés, Spain

11 <sup>4</sup> Museum National d'Histoire Naturelle, Centre de Recherche sur la Paléobiodiversité et les  
12 Paléoenvironnements (CR2P), 75005 Paris, France

13

14 \* Corresponding author : [jorge.cubo\\_garcia@upmc.fr](mailto:jorge.cubo_garcia@upmc.fr)

15

16 RH – Bone histology of *Iberosuchus*

17 **ABSTRACT**

18 *Iberosuchus macrodon* is a Cenozoic crocodyliform interpreted as a terrestrial, cursorial form. In  
19 order to assess if this adaptation was accompanied by a high growth rate and an elevated resting  
20 metabolic rate (two features commonly attributed to several terrestrial Triassic Crocodylomorpha  
21 based on histology) we studied bone histology in the femora of two specimens attributed to *I.*  
22 *macrodon*. Beyond this question is the broader problem of the possible survival to the Cretaceous-  
23 Paleogene extinction event of tachymetabolic sauropsids other than birds. At mid-diaphysis, bone  
24 cortices in *Iberosuchus* are made of a parallel-fibered tissue that turns locally to true lamellar bone.  
25 Cortical vascularization consists of simple longitudinal canals forming a network of medium density.  
26 The spacing pattern of conspicuous lines of arrested growth suggests asymptotic growth for  
27 *Iberosuchus*. This general histological structure prevails also in the metaphyseal region of the bones. It  
28 is basically similar to that encountered in certain large lizards adapted to active predation, the  
29 Varanidae and the Teiidae. In one of the two *Iberosuchus* femora, however, an intra-cortical meniscus  
30 made of a tissue displaying a global radial architecture, occurs in the region of the fourth trochanter.  
31 Histologically, the latter can be interpreted either as compacted spongiosa, or as a fibro-lamellar  
32 complex with a gross radial orientation, a tissue corresponding to fast periosteal apposition. These  
33 observations suggest that, *Iberosuchus* basically had a slow, cyclical growth indicative of an ecto-  
34 poikilothermic, lizard-like, resting metabolic rate. However it might also have retained a limited  
35 capacity for fast periosteal accretion in relation to local morphogenetic requirements as, for instance,  
36 the development of crests or trochanters.

37 Key-words: Crocodylomorphs, Cretaceous-Paleogene extinction event, terrestriality, bone  
38 structure, growth, metabolism.

39

## 40 INTRODUCTION

41 The presence of a four-chambered heart in crocodiles and birds (Seymour *et al.* 2004, Summers  
42 2005) and unidirectional air flow through the lungs (Farmer & Sanders 2010) suggests that the last  
43 common ancestor of archosaurs was endothermic, and that this character state was inherited by  
44 Ornithodira (pterosaurs and dinosaurs including birds) and Pseudosuchia (taxa more closely related to  
45 crocodiles than to birds), but was lost somewhere during the evolution of the latter (Seymour *et al.*  
46 2004). Indirect evidence for this hypothesis has been gained from inferences of bone growth rates of  
47 extinct archosaurs (Ricqlès *et al.* 2008; Cubo *et al.* 2012; Legendre *et al.* 2013), assuming a direct  
48 relationship between bone growth rates and resting metabolic rates (Montes *et al.* 2007). Recently,  
49 resting metabolic rates of extinct archosaurs and non-archosaurian Archosauromorpha were inferred  
50 using bone paleohistology (Legendre *et al.* 2016), providing more direct support for that hypothesis.

51 Interestingly, within Pseudosuchia, aquatic (Dyrosauridae), semiaquatic (Eusuchia) and terrestrial  
52 (Sebecidae and other Sebecosuchia such as *Iberosuchus*) forms survived the Cretaceous-Paleogene  
53 extinction event (Macleod *et al.* 1997). According to the null hypothesis, *Iberosuchus* retained resting  
54 metabolic rates similar to those of Triassic terrestrial Pseudosuchia with an upright stance, such as  
55 *Terrestrisuchus* (Ricqlès *et al.* 2003). Two alternative hypotheses will be tested: (1) The inferred  
56 cursorial locomotion (Riff & Kellner 2011) of *Iberosuchus* suggests that it might have acquired even  
57 higher resting metabolic rates than its Triassic terrestrial relatives. (2) The Cretaceous-Paleogene  
58 extinction event filtered the diversity of Pseudosuchia, so that only taxa showing low resting metabolic  
59 rates survived. Bone histology has been acknowledged for several decades as one of the major clues  
60 for assessing the gross physiological adaptations of extinct taxa (Ricqlès 1974, 1978); unfortunately,  
61 there is no description of the histological features of long bones in notosuchians up to now (only  
62 osteoderms in some taxa were studied; cf. Buffrénil *et al.* 2015). In order to settle the question, we  
63 analyzed the bone histology of *Iberosuchus*, and tentatively interpreted it in terms of growth rates and  
64 metabolism activity.

65

## 66 MATERIAL AND METHODS

67 We analyzed two partial femora assigned to *Iberosuchus macrodon* Antunes 1975 from the  
68 Paleocene of La Boixedat (Spain). These specimens belong to the paleontological collections of the  
69 Institut Català de Paleontologia (ICP), labeled IPS4930 and IPS4932. In contrast to the condition in  
70 the Eusuchia, the femora of *Sebecus* and *Iberosuchus* are (a) straighter and (b) the medial edge of the  
71 greater trochanter is a prominent, sharp, longitudinal crest (Pol *et al.* 2012). Although the specimens in  
72 this study cannot be attributed unequivocally to *Iberosuchus* (whose holotype is a skull fragment), the  
73 morphological congruence of available specimens nevertheless justifies the assumption that the scarce,  
74 non-neosuchian Meoseucrocodylia specimens from the Paleogene of the Iberian Peninsula and  
75 southern France are at least closely related, indistinguishable forms (Ortega *et al.* 1996). We follow  
76 the phylogeny of Pol *et al.* (2012) in which Neosuchia and Notosuchia are sister taxa and *Iberosuchus*  
77 is a sebecosuchian nested in Notosuchia.

78 After photography, the bones were embedded under vacuum in a polyester resin, and two  
79 transverse slices, 3 mm in thick, were removed from the middle of the diaphysis (Fig. 1A, B) and the  
80 base of the proximal metaphysis (Fig. 1E, F) of each femur. According to standard ground section  
81 procedures (e.g. Lamm 2013), these slices were polished on one side, glued on glass slides and  
82 grounded to a thickness  $100\ \mu\text{m} \pm 20$ . These thin sections were observed and photographed with a  
83 Nikon Eclipse E600POL microscope, under normal and cross-polarized light, with or without a  
84 lambda compensator.

85 Simple morphometric measurements were also performed on binary (black and white) images of  
86 the sections at mid-diaphysis (Fig. 1C, D) using the software Image J (Schneider *et al.* 2012). These  
87 measurements include: a) the compactness of each section, or GC (ratio, expressed in percent, of the  
88 area actually occupied by bone tissue to the total sectional area); b) compactness of the cortex proper,  
89 or CC (ratio, expressed in percent, of the actual area of the cortex occupied by bone tissue to the total  
90 cortical area, including bone plus cavities); c) the cortico-diaphyseal index, or CDi (mean thickness of  
91 bone cortex as a fraction of the mean diaphyseal radius).

## 92 RESULTS

### 93 Diaphyseal region of the femora

94 Both femoral diaphyses have a tubular morphology, with a free medullary cavity surrounded by a  
95 compact cortex. However, specimen IPS 4930, though smaller than IPS 4932 (38 % less cross  
96 sectional area) is clearly more compact (GC = 87.16% vs 77.52%) and has a thicker (CDi = 0.65 vs  
97 0.54) and more compact (CC = 99.41% vs 79.06%) cortex. Perimedullary resorption is limited in this  
98 specimen; as a consequence bone layers deposited in early ontogenetic stages are preserved.

99 Histologically, the bone forming the diaphyseal cortex has similar characteristics in the two  
100 specimens. Most of its volume is predominantly composed of parallel-fibered tissue (Fig. 1A, B; Fig.  
101 2A, B), displaying mass birefringence and collagen fiber bundles oriented circularly (i.e. parallel to the  
102 outer contours of the bones). In IPS 4932, this tissue can locally turn to the lamellar type (Fig. 2B).  
103 Frequent irregularities in the birefringence properties of the parallel-fibered bone suggest some degree  
104 of local variation in fiber orientation. Cell lacunae in this tissue are oriented parallel to the collagen  
105 fibers, and they display a small size, as compared to the lacunae occurring in primary or secondary  
106 endosteal deposits forming e.g. osteons (Fig. 2C).

107 The vascularization of the primary cortex mainly consists of simple vascular canals oriented  
108 longitudinally and, to a much lesser extent, obliquely. These canals are relatively few in the peripheral  
109 (outer) part of the cortex; especially in IPS 4932 (Fig. 2A, B). Vascular density increases in deeper  
110 cortical parts, a process much more pronounced in IPS 4930 (Fig. 1B; Fig. 2D) than in IPS 4932 (Fig.  
111 1A). In both specimens, the cortical region bordering the medullary cavity has undergone Haversian  
112 remodeling. This process was relatively diffuse in IPS 4932, where it created sparse secondary osteons  
113 (Fig. 2C, E); it was more restricted but more intense in IPS 4930 where dense Haversian bone tissue  
114 was spatially limited (Fig. 2F). Superficial resorption/reconstruction processes of variable intensity  
115 also occurred around the medullary cavity, creating endosteal layers of secondary lamellar bone.

116 In both specimens the femoral cortex shows cyclical growth marks in the form of lines of arrested  
117 growth (LAGs). The latter appear as thin dark lines parallel to the contour of the bones (Fig. 2G).  
118 These lines are broadly, but unevenly, spaced in the depth of the cortex (280  $\mu$ m in the average on Fig.  
119 2G). In IPS 4932, the spacing of the LAGs suddenly becomes more regular and much narrower in the  
120 most peripheral cortical layers, where the intervals between consecutive LAGs drop to 78  $\mu$ m in the

121 average (Fig. 2G). Both femora also have bundles of short Sharpey's fibers (length  $50\ \mu\text{m} \pm 10$ )  
122 oriented radially and obliquely (Fig. 2H).

### 123 **Histology of the metaphyseal region**

124 The histological structure of primary periosteal cortices in the metaphyseal region of both  
125 specimens (Fig. 1E, F) is basically similar to that prevailing in the diaphyseal region: most of the  
126 cortical volume consists of parallel-fibered bone, the collagen fibers of which are oriented circularly  
127 (Fig. 3A, B). However, three main differences exist. 1) Bone vascularization, mainly represented by  
128 simple vascular canals and primary osteons oriented longitudinally, tends to be lower in the  
129 metaphyses than in the diaphyses, especially in IPS 4930 (Fig. 3A, B). 2) Loose networks of  
130 remodeled endosteal bone trabeculae (Fig. 1E, F; Fig. 3C) partly fill the medullary cavity (the  
131 medullary cavity is free in the diaphysis). 3) In IPS 4932, the cortex is not only composed of  
132 vascularized parallel-fibered tissue; but also contains a broad, central crescent-like meniscus formation  
133 displaying different histological features (Fig. 1F; Fig. 3D). This formation is briefly described below.

134 This peculiar bone layer is located under the forth trochanter of the femur and consequently, it  
135 occupies only a part of the sectional area (Fig. 1F). It is inserted in the middle of the cortex, between  
136 two layers (under and above it) of ordinary parallel-fibered bone (Fig. 3D). Histologically, the thinnest  
137 parts of this meniscus consist merely of some big longitudinal primary osteons (Fig. 3E). In its thicker  
138 part, the meniscus displays two components: 1) Multiple oblong areas made of brightly birefringent  
139 parallel-fibered tissue (blue in Fig. 3F, G) with a dominant, though variable, radial orientation  
140 (including for cell lacunae) and vascular canals also displaying a gross radial orientation. 2) Small and  
141 irregular monorefringent, or poorly birefringent areas, unevenly wedged between the birefringent  
142 ones, and formed by woven bone (red in Fig. 3F, G). They contain big multipolar cell lacunae.

143 This basic structure can be interpreted in two distinct ways. The first interpretation is that it  
144 represents former spongiosa, compacted by endosteal deposits. Crests, trochanters and other bone  
145 excrescences related to muscle insertion are most often associated with spongy tissues within bone  
146 cortices (e.g. Ricqlès 1976a). During growth, such spongiosae are frequently made compact by inter-  
147 trabecular filling, a situation actually observed by one of us (VB) in sections of the fourth trochanter

148 of two alligatorids, *Alligator mississippiensis* and *Diplocynodon ratelii*. The gross radial orientation  
149 of this compacted spongiosa in IPS 4932 reflects the strong traction stress exerted on the periosteum  
150 and the growing bone cortex by the muscle *caudofemoralis* (according to Wolf's law; cf. Currey  
151 2002). An alternative interpretation of the meniscus structure is that it is made of a radiating fibro-  
152 lamellar bone complex, a tissue known to be characteristic of fast or very fast accretion. The  
153 monorefringent areas would represent the woven-fibered trabeculae initially deposited by the  
154 periosteum. The brightly birefringent areas would be primary osteons. The main difference between  
155 the bone forming the meniscus and typical fibro-lamellar complexes is that the highly ordered and  
156 conspicuous periosteal scaffoldings of woven-fibered trabeculae that characterize these complexes  
157 cannot be clearly identified in *Iberosuchus*. As a consequence, the limits and shape of the putative  
158 primary osteons cannot be traced precisely. For this reason, the tissue forming the thick part of the  
159 meniscus should be interpreted, with necessary caution, as an atypical form of radial fibro-lamellar  
160 bone tissue. Both interpretations, compacted spongiosa vs radiating fibro-lamellar complex, differ  
161 little from each other. In both cases, the differentiation of the fourth trochanter basically involves the  
162 sub-periosteal accretion of a spongiosa, and its subsequent compaction by inter-trabecular, centripetal  
163 deposits of endosteal lamellar or parallel-fibered tissue. Their main difference would reside in the  
164 dynamics of bone deposits: fast or very fast periosteal and endosteal deposits in the case of a radiating  
165 fibro-lamellar complex; much slower deposits in the case of a compacted spongiosa.

166 The basal part of the meniscus is in continuity (though histologically very distinct) with the  
167 subjacent parallel-fibered tissue. Conversely, the peripheral border of the meniscus is marked by a  
168 reversion line displaying a typical scalloped contour at high magnification (Fig. 3H). Above this line,  
169 towards bone periphery, the parallel-fibered tissue prevails again. The occurrence of this reversion line  
170 means that, during growth, the height of the basal part of the trochanter had to be reduced, through a  
171 resorption process, to become compatible with the diameter of the diaphysis into which the trochanter  
172 was sequentially relocated.

## 173 DISCUSSION

174 The most significant result of this study is that the femoral cortex of *Iberosuchus* is made of a  
175 parallel-fibered tissue with variable vascular density and conspicuous lines of arrested growth. This  
176 situation was observed in all bone sections, especially those sampled at mid-diaphysis, i.e. a sectional  
177 plane classically considered as a general reference for histological studies of long bones; e.g. Lamm  
178 2013). This result strongly suggests that *Iberosuchus* was not a fast growing, tachymetabolic animal,  
179 but a slow growing crocodile with steep, cyclic decreases in growth rate. Several experimental studies  
180 indeed show that, on the one hand, bone tissue with scattered longitudinal vascular canals results from  
181 accretion speeds less than 5  $\mu\text{m}/\text{day}$  (Castanet *et al.* 1996) and that, on the other hand, parallel-fibered  
182 bone corresponds to accretion rates less than 1  $\mu\text{m}/\text{day}$  (e.g. Buffr nil & Pascal 1984). The actual  
183 apposition rate on the femoral cortex of *Iberosuchus* could have been between these values which are  
184 anyway far below those prevailing for the woven-fibered tissue, especially when it contributes to the  
185 constitution of fibro-lamellar complexes (laminar, plexiform, radiating bone tissues) typically  
186 encountered in fast growing endotherms (Castanet *et al.* 1996, 2000; Margerie *et al.* 2002; see also  
187 Cubo *et al.* 2012). In most modern crocodiles, the femoral cortex is made of a lamellar-zonal tissue  
188 (Enlow & Brown 1957, Ricql s 1976b, Lee 2004) displaying conspicuous yearly growth cycles. The  
189 latter consist of zones made of woven-fibered tissue (that may change to the parallel-fibered type),  
190 associated with annuli made of parallel-fibered or true lamellar bone (Buffr nil 1980a, b; Hutton  
191 1986). These two components of an annual growth cycle are deposited sequentially and reflect a  
192 progressive decrease in growth rate that may end, each year, in a total cessation of growth and the  
193 formation of a LAG (Buffr nil 1980a). Since it integrates a woven-fibered component, the lamellar-  
194 zonal tissue reflects faster deposition than the mere parallel-fibered type prevailing in *Iberosuchus*.  
195 The occurrence of lines of arrested growth in this taxon, as well as the absence of annuli, clearly  
196 shows that the maximum growth rate in *Iberosuchus* was comparable to the slowest rates of modern  
197 crocodiles, and that growth stopped completely each year. As observable in the femur, the histological  
198 features of *Iberosuchus* can be best compared to those of large predatory squamates such as the  
199 varanids or the teids (e.g. Duarte-Varela & Cabrera 2000, Buffr nil & H mery 2002, see also Cubo *et*  
200 *al.* 2014). In both cases, bone cortices are made of parallel-fibered tissue (that may turn to the woven-  
201 fibered type in the inner cortex) comprising longitudinal simple vascular canals or primary osteons,

202 and lines of arrested growth. Therefore, if the histological structure of long bones indeed reflects  
203 growth rate, as initially proposed by Amprino (1947) and universally acknowledged today, then the  
204 growth activity of *Iberosuchus* should be considered similar to that of extent large lizards. This  
205 comparison is further substantiated by the spacing pattern of cyclical growth marks in IPS 4932.  
206 Growth mark spacing indeed suggests that a sudden and steep decrease in growth activity occurred  
207 about six years before this animal died. Its growth pattern was thus clearly asymptotic, a situation  
208 commonly encountered in squamates in which epiphyseal and metaphyseal fusion limits growth  
209 possibilities (Maisano 2008, Buffrénil *et al.* 2004). Conversely, this growth pattern is unusual in  
210 crocodiles, though it was observed in some populations of *Alligator mississippiensis* (Woodward *et al.*  
211 2011; see also Lee *et al.* 2013). IPS 4932 is larger than IPS 4930 and displays signs of a sudden  
212 decrease in growth. These two characteristics indicate an older age for IPS 4932. Moreover, the  
213 porosity of deep cortical layers in this specimen is a feature commonly encountered in mature  
214 crocodylian females (Wink & Elsey 1986; Wink *et al.* 1987).

215 If the general relationship between the histological structure of primary bone cortices and their  
216 appositional rate is now strongly evidenced by experimental data (e.g. Castanet *et al.* 1996), the  
217 association between, on the one hand, bone tissue types and growth rate and, on the other hand, the  
218 resting metabolic rate of an organism, seems to be less simple and less clearly deciphered. Montes *et*  
219 *al.* (2007) found a direct relationship between periosteal bone growth rate and resting metabolic rate in  
220 a sample of growing amniotes. In general, long bone cortices made of parallel-fibered tissue, be it  
221 vascularized or not, are characteristically encountered in ecto-poikilothermic tetrapods (e.g. Enlow and  
222 Brown 1956-1958, Ricqlès 1976). However, the few extant large squamates displaying vascular canals  
223 (simple canals or primary osteons) within parallel-fibered bone, i.e. the largest Teiidae (Duarte-Varela  
224 & Cabrera 2000, Cubo *et al.* 2014) and the Varanidae more than 30 cm in snout-vent length (Buffrénil  
225 *et al.* 2008), can experience transitory episodes of relatively high and constant metabolic rate during  
226 either their reproductive cycle (Tattersall *et al.* 2016), or during times of intense foraging activity  
227 (synthesis in Thompson 1999). Otherwise, these animals, including the largest ones, have a typical  
228 ecto-poikilothermic physiology (Green *et al.* 1991, Christian & Conley 1994, Wikramanayake *et al.*

229 1999). The question is made more complex by the fact that the very same type of bone tissue  
230 (vascularized parallel-fibered bone) can be observed in long bone cortices in some large anurans, such  
231 as *Rana Catesbeiana*, *Rhinella marina*, or *Pipa pipa* (pers. obs. VB), known to have much lower  
232 metabolic rates than the squamates in general (White et al. 2006 ). Such observations suggest that the  
233 actual relationship between the details of bone structure and the metabolic rate of an organism result  
234 from a complex, multifactorial causality that needs to be fully deciphered. It nevertheless remains that  
235 bone cortices mainly composed of parallel-fibered tissue are very unlikely to belong to an endotherm-  
236 homeotherm animal. For this reason, the fundamental thermal regime of *Iberosuchus* should be  
237 considered to have been ectotherm and poikilotherm, as is also the case for the large extant squamates  
238 or lissamphibians mentioned above.

239 The particular case of *Iberosuchus* suggests that, in pseudosuchians, a terrestrial habitat is not  
240 necessarily associated with a high, sustained growth speed and the tachymetabolic regime consistent  
241 with it. Of course, this conclusion holds only for *Iberosuchus*. The Notosuchia (of which the  
242 Sebecosuchia are but one clade) represent a particularly rich and diversified lineage of terrestrial forms  
243 in which a number of bizarre and ecologically enigmatic taxa occur (e.g. Ortega *et al.* 2000). Future  
244 comparative studies should document whether this high morphological diversity also involved  
245 significant physiological discrepancies.

246 One element in our observations could challenge the conclusion presented above: the possible  
247 occurrence of radiating fibro-lamellar tissue in a limited area of the metaphyseal cortex of IPS 4932.  
248 This type of bone tissue is considered to result from the fastest accretion rate (Margerie *et al.* 2004)  
249 and is supposed to be an exclusive feature of fast-growing tachymetabolic tetrapods (Ricqlès 1974,  
250 1976a). For several reasons, the occurrence of radiating fibro-lamellar tissue in the core of the  
251 metaphyseal cortex cannot be alleged to conclude that (1) episodes of fast growth occurred in the life  
252 of IPS 4932, and (2) that this taxon had the physiological competence for sustaining them at the level  
253 of the organism as a whole. As mentioned in the observations, the identification of this tissue is  
254 debatable, due to atypical histological characteristics. Nevertheless, even if the tissue forming the  
255 meniscus is really akin to fibro lamellar radiating bone, the complete lack of this tissue in diaphyseal

256 cortices (despite the excellent preservation of primary cortical tissues) would clearly indicate that its  
257 occurrence in the proximal metaphysis of IPS 4932 does not indicate a general trend towards fast  
258 growth in *Iberosuchus*, but a local, topographically restricted, process. This taxon might indeed have  
259 retained the potential capacity to develop fast periosteal accretion but, in the specimen studied here,  
260 this capacity would have been expressed in a strictly local context, in relation to the differentiation,  
261 growth and sequential relocation of the fourth trochanter during ontogeny.

262 With reference to the hypotheses listed in the introduction, our results suggest that the situation  
263 may be more complex than expected because some crocodyliforms might have preserved  
264 physiological potentialities that could have been expressed, or non-expressed, depending on  
265 morphological and/or ecological contexts. Future studies based on larger samples should settle more  
266 firmly this interesting question, and help assess if the capacity for fast growth, at least in limited  
267 skeletal regions and for a limited duration, is a frequent feature in the Notosuchia.

#### 268 LITERATURE CITED

269 Amprino, R. 1947: La structure du tissu osseux envisagée comme expression de différences dans la  
270 vitesse de l'accroissement. *Archives de Biologie* 58, 315–330.

271 Antunes, M.T. 1975: *Iberosuchus*, crocodile Sébécosuchien nouveau, de l'Eocène ibérique au Nord  
272 de la Chaîne centrale, et l'origine du canyon de Nazaré. *Comunicações dos Serviços Geológicos de*  
273 *Portugal* 59, 285-330.

274 Antunes, M.T. 1986: *Iberosuchus* et *Pristichampsus*, crocodiliens de l'Eocène : données  
275 complémentaires, discussion, distribution stratigraphique. *Ciências da Terra* 8, 111-122.

276 Buffrénil, V. de. 1980a: Données préliminaires sur la structure des marques de croissance  
277 squelettiques chez les crocodiliens actuels et fossiles. *Bulletin de la Société Zoologique de France*  
278 105, 355-361.

279 Buffrénil, V. de. 1980b: Mise en évidence de l'incidence des conditions de milieu sur la croissance  
280 de *Crocodylus siamensis* (Schneider, 1801) et valeur des marques de croissance squelettiques pour  
281 l'évaluation de l'âge individuel. *Archives de Zoologie Expérimentale et Générale* 121, 63-76.

282 Buffrénil, V. de & Pascal, M. 1984: Croissance et morphogénèse postnatales de la mandibule du  
283 vison (*Mustela vison* Schreiber) : données sur la dynamique et l'interprétation fonctionnelle des dépôts  
284 osseux mandibulaires. *Canadian Journal of Zoology* 62, 2026-2037.

285 Buffrénil, V. de & Castanet, J. 2000 : Age estimation by skeletochronology in the Nile monitor  
286 (*Varanus niloticus*), a highly exploited species. *Journal of Herpetology* 34, 414-424.

287 Buffrénil, V. de & Hémerly, G. 2002: Variation in longevity, growth, and morphology in exploited  
288 Nile monitors (*Varanus niloticus*) from sahelian Africa. *Journal of Herpetology* 36, 419-426.

289 Buffrénil, V. de, Ineich, I. & Böhme, W. 2004: Comparative data on epiphyseal development in the  
290 family Varanidae. *J. Herpetology* 37, 328-335.

291 Buffrénil, V. de, Clarac, F., Fau M., Martin, S., Martin B., Pellé, E. & Laurin, M. 2015:  
292 Differentiation and growth of bone ornamentation in vertebrates: a comparative histological study  
293 among the Crocodylomorpha. *Journal of morphology* 276, 425-445.

294 Castanet, J., Grandin, A., Abourachid, A., & Ricqlès, A. de. 1996: Expression de la dynamique de  
295 croissance dans la structure de l'os périostique chez *Anas platyrhynchos*. *Comptes-Rendus de*  
296 *L'Académie des Sciences, Paris, Sciences de la Vie* 319, 301-308.

297 Castanet, J., Curry-Rogers, K., Cubo, J. & Boisard, J-J. 2000: Periosteal bone growth rates in  
298 extant ratites (ostrich and emu). Implications for assessing growth in dinosaurs. *Comptes-Rendus de*  
299 *L'Académie des Sciences, Paris, Sciences de la Vie* 323, 543-550.

300 Christian, K.A. & Conley, K.E. 1994: Activity and resting metabolism of varanid lizards compared  
301 with "typical" lizards. *Australian Journal of Zoology* 42, 185-193.

302 Cubo, J., Le Roy, N., Martinez-Maza, C., Montes, L. 2012: Paleohistological estimation of bone  
303 growth rate in extinct archosaurs. *Paleobiology* 38, 335-349.

304 Cubo, J., Baudin, J., Legendre, L., Quilhac, A., Buffrénil, V. de 2014: Geometric and metabolic  
305 constraints on bone vascular supply in diapsids. *Biological Journal of the Linnean Society of London*  
306 112, 668-677.

307 Duarte-Varela, C.F. & Cabrera, M.R. 2000: Testing skeletochronology in black tegu lizards  
308 (*Tupinambis merianae*) of known ages. *Herpetological Review* 31, 224-226.

309 Enlow, D.H. & Brown, S.O. 1957: A comparative histological study of fossil and recent bone tissues.  
310 Part II. *Texas Journal of Science* 9, 186-214.

311 Farmer, C.G. and Sanders, K. 2010: Unidirectional Airflow in the Lungs of Alligators. *Science*  
312 327, 338–340.

313 Green, B., King, D., Braysher, M., & Saim, A. 1991: Thermoregulation, water turnover and  
314 energetics of free-ranging Komodo dragons, *Varanus komodoensis*. *Comparative Biochemistry and*  
315 *Physiology* 99A, 97-101.

316 Hutton, J.M. 1986: Age determination of living Nile crocodiles from the cortical stratification of  
317 bone. *Copeia* 1986(2), 332-341.

318 Lamm, E.-T. 2013: Preparation and sectioning of specimens. In Padian, K., Lamm, E.-T. (eds): *Bone*  
319 *Histology of Fossil Tetrapods*, 55–160. University of California Press, Berkeley.

320 Lee, A.H. 2004: Histological organization and its relationship to function in the femur of *Alligator*  
321 *mississippiensis*. *Journal of Anatomy* 204, 197-207.

322 Legendre, L.J., Segalen, L. and Cubo, J. 2013: Evidence for high bone growth rate in *Euparkeria*  
323 obtained using a new paleohistological inference model for the Humerus. *Journal of Vertebrate*  
324 *Paleontology* 33, 1343–1350.

325 Legendre, L.J., Guénard, G., Botha-Brink, J. and Cubo, J. 2016: Paleohistological evidence for  
326 ancestral high metabolic rate in archosaurs. *Systematic Biology* 65, 989-996.

327 Macleod, N., Rawson, P.F., Forey, P.L., Banner, F.T., BoudagherFadel, M.K., Bown, P.R.,  
328 Burnett, J.A., Chambers, P., Culver, S., Evans, S.E., Jeffery, C., Kaminski, M.A., Lord, A.R., Milner,  
329 A.C., Milner, A.R., Morris, N., Owen, E., Rosen, B.R., Smith, A.B., Taylor, P.D., Urquhart, E. and  
330 Young, J.R. 1997: The Cretaceous-Tertiary biotic transition. *Journal of the Geological Society* 154,  
331 265–292.

332 Maisano, J.A. 2002: Terminal fusion of skeletal elements as indicators of maturity in squamates.  
333 *Journal of Vertebrate Paleontology*, 22, 268-275.

334 Margerie, E. de, Cubo, J. & Castanet, J. 2002: Bone typology and growth rate: testing and  
335 quantifying « Amprino's rule » in the mallard (*Anas platyrhynchos*). *Comptes-Rendus de. L'Académie*  
336 *des Sciences, Paris, Sciences de la Vie* 325, 221-230.

337 Margerie, E. de, Robin, J-P., Verrier, D., Cubo, J. & Groscolas, R. 2004: Assessing the  
338 relationship between bone microstructure and growth rate: a fluorescent labelling study in the king  
339 penguin chick (*Aptenodytes patagonicus*). *Journal of Experimental Biology* 207, 869-879.

340 Montes, L., Le Roy, N., Perret, M., Buffrénil, V. de, Castanet, J. & Cubo, J. 2007: Relationship  
341 between bone growth rate, body mass and resting metabolic rate in growing amniotes: a phylogenetic  
342 approach. *Biological Journal of the Linnean Society* 92, 63-76.

343 Ortega, F., Buscalioni, A.D. and Gasparini, Z. 1996: Reinterpretation and new denomination of  
344 *Atacisaurus crassiproratus* (Middle Eocene; Issel, France) as cf *Iberosuchus* (Crocodylomorpha,  
345 Metasuchia). *Geobios* 29, 353–364.

346 Ortega, F., Gasparini, Z., Buscalioni, A.D. and Calvo, J.O. 2000: A new species of *Araripesuchus*  
347 (Crocodylomorpha, Mesoeucrocodylia) from the Lower Cretaceous of Patagonia (Argentina). *Journal*  
348 *of Vertebrate Paleontology* 20, 57–76.

349 Pol, D., Leardi, J.M., Lecuona, A. and Krause, M. 2012: Postcranial Anatomy of *Sebecus*  
350 *Icaeorhinus* (crocodyliformes, Sebecidae) from the Eocene of Patagonia. *Journal of Vertebrate*  
351 *Paleontology* 32, 328–354.

352 Ricqlès, A. de. 1974: Evolution of endothermy: histological evidence. *Evolutionary Theory* 1, 51-  
353 80.

354 Ricqlès, A. de. 1976a: Recherches paléohistologiques sur les os longs des tetrapodes. VII. – Sur la  
355 classification, la signification fonctionnelle et l'histoire des tissus osseux des tetrapodes. *Annales de*  
356 *Paléontologie* 62, 71-126.

357 Ricqlès, A. de. 1976b: On bone histology of fossil and living reptiles, with comments on its  
358 functional and evolutionary significance. In Bellairs, A. d'A. & Cox, C.B. (eds) *Morphology and*  
359 *Biology of Reptiles*, 123-150. Linnean society Symposium Series n°3, London.

360 Ricqlès, A. de. 1978: Recherches paléohistologiques sur les os longs des tétrapodes. VII. – Sur la  
361 classification, la signification fonctionnelle et l’histoire des tissus osseux des tétrapodes (troisième  
362 partie). *Annales de Paléontologie* 64, 85-111.

363 Ricqlès, Ad., Padian, K. & Horner, J.R. 2003: On the bone histology of some Triassic  
364 pseudosuchian archosaurs and related taxa. *Annales de Paléontologie* 89, 67–101.

365 Ricqlès, A. de, Padian, K., Knoll, F., Horner, J.R. 2008: On the origin of high growth rates in  
366 archosaurs and their ancient relatives: Complementary histological studies on Triassic archosauriforms  
367 and the problem of a “phylogenetic signal” in bone histology. *Annales de Paléontologie* 94, 57-76.

368 Riff, D. and Armin Kellner, A.W. 2011: Baurusuchid crocodyliforms as theropod mimics: clues  
369 from the skull and appendicular morphology of *Stratiosuchus maxhecti* (Upper Cretaceous of  
370 Brazil). *Zoological Journal of the Linnean Society* 163, S37–S56.

371 Schneider, C.A. Rasband, W.S. and Eliceiri, K.W. 2012 : [NIH Image to ImageJ: 25 years of image](#)  
372 [analysis](#). *Nature methods* 9(7), 671-675.

373 Seymour, R.S., Bennett-Stamper, C.L., Johnston, S.D., Carrier, D.R. and Grigg, G.C. 2004:  
374 Evidence for endothermic ancestors of crocodiles at the stem of archosaur evolution. *Physiological*  
375 *and Biochemical Zoology* 77, 1051–1067.

376 Summers, A.P. 2005: Evolution - Warm-hearted crocs. *Nature* 434, 833–834.

377 Tattersall, G.J., Leite, C.A.C., Sanders, C.E., Cadena, V., Andrade, D.V., Albe, A.S., Milson, W.K.  
378 2016 : Seasonal reproductive endothermy in Tegu lizards. *Scientific Advances* 2016 ; e1500951.

379 Thompson, G. 1999 : Goanna metabolism : different to other lizards, and if so, what are the  
380 ecological consequences ? In Horn, H.-G. & Böhme, W. (eds.) *Advances in monitor research II. –*  
381 *Mertensiella* 11, 79-90.

- 382 Wink, C.S. & Elsey, R.M. 1986: Changes in femoral morphology during egg-laying in *Alligator*  
383 *mississippiensis*. *Journal of Morphology* 189, 183-188.
- 384 Wink, C.S., Elsey, R.M. & Hill, E.M. 1987: Changes in femoral robusticity and porosity during the  
385 reproductive cycle of the female Alligator (*Alligator mississippiensis*). *Journal of Morphology* 193:  
386 317-321.
- 387 White, C.R., Phillips, N.F., Seymour, R.S. 2006 : The scaling and temperature dependence of vertebrate  
388 metabolism. *Biology Letters* 2, 125-127.
- 389 Wikramanayake, E.D, Ridwan, W. & Marcellini, D. 1999 : The thermal ecology of free-ranging  
390 Komodo dragons, *Varanus komodoensis*, on Komodo Island, Indonesia. In Horn, H.-G. & Böhme, W.  
391 (eds.) Advances in monitor research II. – *Mertensiella* 11, 157-166.
- 392 Woodward, H.N., Horner, J.R. & Farlow, J.O. 2011: Osteohistological evidence for determinate  
393 growth in the American alligator. *Journal of Herpetology* 45, 339-342.

394

#### 395 ACKNOWLEDGEMENTS

396 We thank Francisco Ortega for his valuable help in performing the taxonomic assignment of  
397 the samples analyzed to *Iberosuchus*. We would like to express our gratitude to an anonymous  
398 reviewer for his/her helpful comments and to an associate editor for his/her stylistic suggestions. This  
399 work was supported by the Spanish Ministry of Economy and Competitiveness: CGL2015-63777-P,  
400 PI: MK, and 2014 SGR 1207, PI: MK, and [CERCA Programme / Generalitat de Catalunya](#). We have  
401 no conflict of interest to declare.

402

#### 403 FIGURE LEGENDS

404 Figure 1: Gross aspect of the sections.

405 A: Global aspect of the the mid-diaphyseal section in IPS 4930. B: Global aspect of the the mid-  
406 diaphyseal section in IPS 4932. C: Binary image of the mid-diaphyseal section in specimen IPS 4930.

407 D: Binary image of the mid-diaphyseal section in specimen IPS 4932. E: Global aspect of the the  
408 metaphyseal section in IPS 4930. F: Global aspect of the metaphyseal section in IPS 4932. Scale bar: 2  
409 mm.

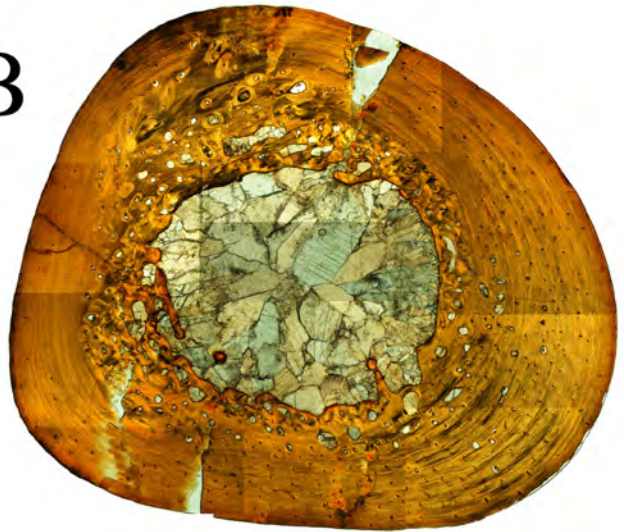
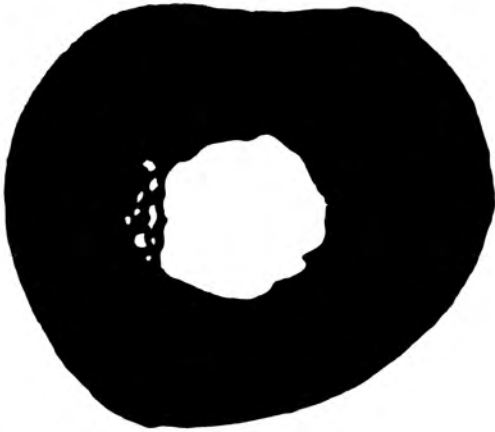
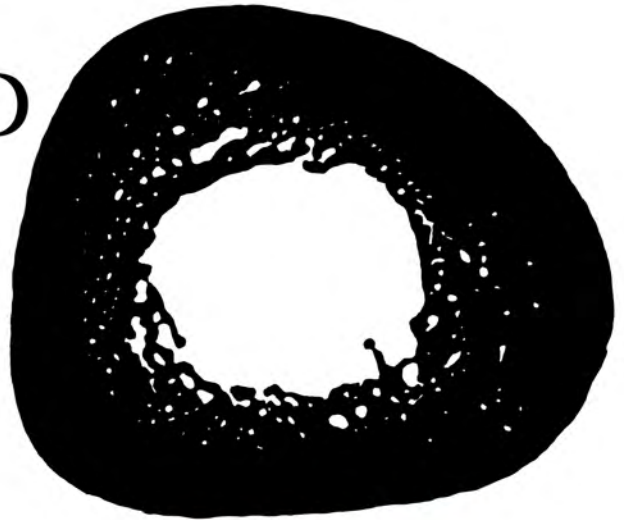
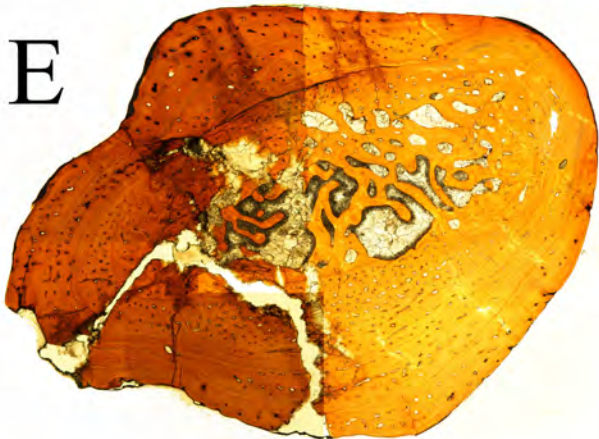
410 Figure 2: Bone histology in the femoral diaphysis in IPS 4930 and 49832.

411 A: Peripheral cortex of the femur in IPS 4930. The upper part is viewed in transmitted polarized  
412 light with lambda compensator; the lower part in ordinary transmitted light. B: Peripheral cortex of the  
413 femur in IPS 4932. Upper part: transmitted polarized light with lambda compensator; lower part:  
414 ordinary light. C: Size of osteocyte lacunae in periosteal and endosteal deposits (IPS 4932). The insert  
415 is a closer view at the wall of a secondary osteon as compared to the primary periosteal cortex. D:  
416 vascular density in the deep, peri-medullary cortex of IPS 4930. E: Secondary osteons scattered in the  
417 cortex of specimen IPS 4932. Polarized light. F: Localized area of dense Haversian tissue around the  
418 medullary cavity in IPS 4930. G: Lines of arrested growth, or LAG (arrows) in the cortex of IPS 4932.  
419 Note the tight spacing of the last LAGs. H: Sharpey's fibers in the cortex of IPS 4930 (arrows). All  
420 scale bars are equal to 0.5 mm but that of the close-up in C, which equals 0.1 mm.

421 Figure 3: Histological characteristics of the metaphyseal region.

422 A: Basic appearance of the femoral cortex in the metaphyseal region of IPS 4930. Upper part:  
423 transmitted polarized light with lambda compensator; lower half: ordinary transmitted light. B:  
424 Femoral cortex in the metaphyseal region of IPS 4932. Upper part: transmitted polarized light with  
425 lambda compensator; lower half: ordinary transmitted light. C: Remodeled endosteal trabeculae  
426 occupying the medullary cavity in the metaphysis of IPS 4930. Polarized light. D: Complex cortical  
427 structure observed locally in the metaphyseal of IPS 4932. The inner (left) and the outer (right) parts  
428 of the cortex are formed by parallel-fibered bone, the collagen fibers of which are oriented circularly  
429 (yellow). In between these layers the cortex is occupied by a tissue with a dominant radial  
430 structuration. E: Longitudinal primary osteons in the thin extremities of the crescent-like meniscus.  
431 Polarized light. F: Complex histological organization in the thick parts of the meniscus. Brightly  
432 birefringent (here in blue) and poorly birefringent (here in red) areas oriented radially are unevenly  
433 inter-mixed. Polarized light with lambda compensator. G: Continuity of the basal, parallel-fibered part

434 of the cortex (bottom part of the picture) with the tissue forming the meniscus. Polarized light with  
435 lambda compensator. H: Reversion line (RL) separating the meniscus and the peripheral layer of  
436 parallel-fibered bone tissue. The insert shows the typical scalloped contour of the reversion line. All  
437 scale bars are equal to 0.5 mm but that of the close-up in H, which equals 0.1 mm.

**A****B****C****D****E****F**